

Amylose Crystallization from Concentrated Aqueous Solution

John A. Creek, Gregory R. Ziegler,* and James Runt

The Pennsylvania State University, 116 Borland Lab, University Park, Pennsylvania 16801

Received October 13, 2005; Revised Manuscript Received December 9, 2005

Maize amylose, separated from granular starch by means of an aqueous leaching process, was used to investigate spherulite formation from concentrated mixtures of starch in water. Amylose (10–20%, w/w) was found to form a spherulitic semicrystalline morphology over a wide range of cooling rates (1–250 °C/min), provided it was first heated to > 170 °C. This is explained through the effect of temperature on chain conformation. A maximum quench temperature of approximately 70 °C was required to produce spherulitic morphology. Quench temperatures between 70 and 110 °C produced a gel-like morphology. This is explained on the basis of the relative kinetics of liquid–liquid phase separation vis-à-vis crystallization. The possibility of the presence of a liquid crystalline phase affecting the process of spherulite formation is discussed.

Introduction

Self-assembly of biological macromolecules is a fertile area of study. Among the morphologies formed through self-assembly are spherulites. Spherulites are semicrystalline entities in which crystal lamellae or fibers are radially oriented, producing a characteristic extinction pattern known as a “Maltese cross” when viewed between crossed polarizers using light microscopy. Radially oriented, chain-folded lamellae result in “negative” spherulites with the main axis of the polymer chains tangential to the radius. Spherulitic self-assembly is observed under certain circumstances for natural polymers including cellulose,¹ DNA,^{2–6} chitin,^{7,8} chitosan,⁹ silk fibroin,¹⁰ collagen,¹¹ and insulin.¹² Some of these spherulites are thought to contain liquid crystals (LCs).^{2,3,5,7,9,11} In the case of starch, spherulites are formed under dynamic, nonequilibrium conditions.

Rigid macromolecules in solution are expected to form liquid crystalline phases beyond a minimum concentration, dependent on the persistence length. The conditions of liquid crystal formation are best met when the polymer has some portion of its structure in the form of rods.¹³ These conditions are met by cellulose and poly(γ -benzyl L-glutamate), which form birefringent, anisotropic phases in lyotropic systems.¹³ In recent years numerous carbohydrate polymers have been found to yield lyotropic mesophases in aqueous environments.¹ Nematic liquid crystals can form emulsions in water that exhibit extinction patterns between crossed polarizers resembling spherulites.¹⁴ Preordering before crystallization can result from long-living or transient metastable states such as liquid crystal phases, which may also provide nuclei for the final crystalline state.¹⁵

Starch is composed of amylose, a linear or lightly branched (1→4)-linked α -glucan of MW 10^5 – 10^6 , and amylopectin, a highly branched molecule of MW 10^7 – 10^9 containing numerous (1→4)-linked α -glucan chains linked α -(1→6). Starch is found in plants as complex structures known as granules that vary in size (1–100 μ m) and shape characteristic of the plant source.¹⁶ The granular structure can be disrupted through the application of heat in the presence of excess moisture (> 70 wt %) in a process called gelatinization. On cooling, the granular structure does not re-form; instead a variety of morphologies may form

including gels and precipitates. In general, the resulting structure will depend on such physical processes as crystallization, vitrification, liquid–liquid demixing, changes in molecular conformation (e.g., coil \leftrightarrow helix), intermolecular association, and combinations of each involving multiple processes occurring in stages.¹⁷

We have reported previously on spherulite formation from native starches.^{18–21} In general, spherulite formation was only possible if starch dispersions were heated to temperatures > 170 °C.²⁰ A minimum concentration for spherulite formation of about 5% starch (w/w) was observed, and spherulite formation was favored in starches containing a greater percentage of linear material and exhibiting B-type X-ray diffraction patterns. Contrary to granular starch, where crystallinity drops with increasing amylose content,²² recrystallization following gelatinization is favored in linear starches.²³ For example, films comprising mixtures of amylose and amylopectin are semicrystalline, the degree of crystallinity increasing with amylose content.²⁴ Linear polymers typically crystallize more readily than their branched counterparts,²⁵ and in synthetic polymers, branched molecules have been shown to hinder spherulite formation.²⁶ When crystallization processes are investigated, it is desirable to begin with relatively simple, linear molecules.^{27,28} Here we investigate the boundaries, both thermodynamic and kinetic, of spherulite formation from maize amylose, with the hope of expanding our understanding of the self-assembly of starch polymers from solution, and hence polymer crystallization in general.

Experimental Section

Materials. Common maize starch was supplied by the National Starch and Chemical Corp. Food Products Division (Bridgewater, NJ). Dimethyl sulfoxide (DMSO) (471267), d_6 -DMSO (151874), and amylopectin (10118, Fluka Biochemika) were purchased from Sigma Aldrich (St. Louis, MO). USP ethyl alcohol (111000200PL05) was obtained from Pharmco (Brookfield, CT).

Amylose was leached from a 4% (w/v) suspension of common maize starch using distilled water at 75 °C with gentle stirring for 45 min.²⁹ The suspension was centrifuged at 2950g and the supernatant reserved. Starch granules were resuspended and leached two more times, after which 1.5 volumes of ethanol was added to the combined supernatants, and the resulting precipitate (collected at 25 °C) was dried at 40 °C.

* To whom correspondence should be addressed. E-mail: grz1@psu.edu.

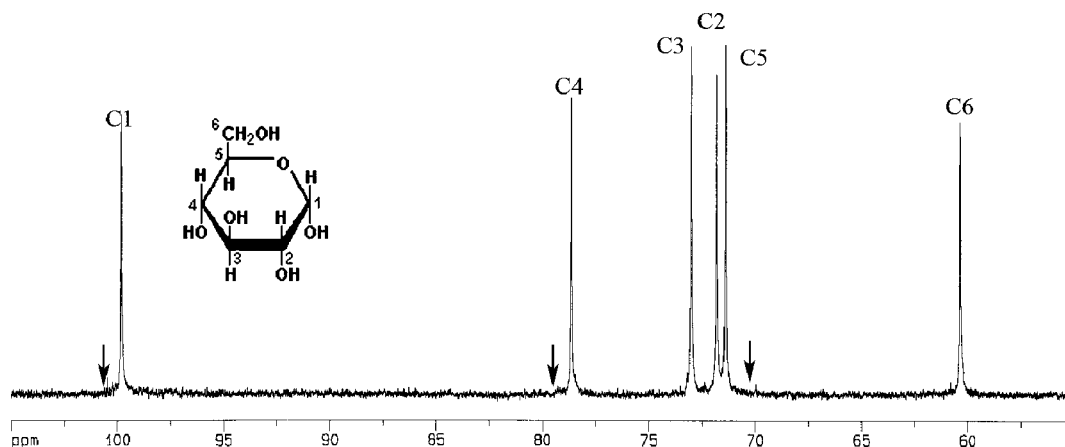


Figure 1. ^{13}C NMR spectrum of the leached starch in d_6 -DMSO. Arrows indicate the expected positions of resonance peaks in a 1,6-branched polysaccharide. The chemical structure indicates glucose carbon assignments.

Amylose was characterized using ^1H and ^{13}C NMR. Approximately 30 mg of amylose was dissolved in 1.5 mL of d_6 -DMSO using a boiling water bath. The ^1H and ^{13}C NMR experiments were performed at 500.13 and 125.76 MHz, respectively, on a Bruker AMX2-500 spectrometer operating in the quadrature mode at 60 °C. ^1H and ^{13}C NMR were referenced indirectly to tetramethylsilane. The generated spectra were compared to previously published starch NMR data. NMR revealed the leached maize fraction to be essentially free of branching as evidenced by the absence of a peak at 70 ppm (Figure 1) that is typical of starch containing 1–6 branch points.^{30,31} Benesi and Brant³² assigned a peak at 70.4 ppm to carbon 4 of the glucose bound at carbon 6 of the 1–6 branch points of pullulan. Therefore, we concluded that the leached maize fraction is essentially amylose, free of amylopectin.

Intrinsic viscosity in DMSO at 25 °C (± 0.1 °C) was determined using a Cannon-Ubbelohde dilution viscometer (no. 50, Cannon Instrument Co., State College, PA). Four concentrations were measured in the range 0.001–0.005 g/mL. Efflux times were recorded in triplicate using a digital stopwatch (Traceable, VWR International, West Chester, PA). Mark–Houwink–Sakurada values (α and K) calculated by Banks and Greenwood (0.70 and 0.0151, respectively)³³ and Everett and Foster (0.64 and 0.0306, respectively)³⁴ for amylose in DMSO were both used to calculate the molecular weight and the results averaged.³⁵ The leached amylose was found to have a viscosity-average molecular weight of 1.5×10^5 , corresponding to a degree of polymerization of approximately 925, which is toward the low end of the molecular weight distribution for maize amylose. However, the final yield of leached material was approximately 6 wt % of the original starch with a moisture content of 12.5% (w/w) when equilibrated at room temperature and 50% relative humidity. This is about $1/5$ to $1/4$ of the total amylose present in the parent starch. In this case we chose to sacrifice yield (and therefore length) to obtain unbranched amylose.

Sample Preparation. Starch suspensions of 10% dry mass in water, determined in previous studies to be ideal for the formation of spherulites,²⁰ were prepared in high-volume (60 μL) stainless steel differential scanning calorimetry (DSC) pans (Perkins-Elmer Instruments, Norwalk, CT). The pans were hermetically sealed and stored overnight at 20 °C to ensure moisture equilibration. Samples were heated to 180 °C at a rate of 10 °C/min and then immediately cooled at various predetermined rates (e.g., 250, 100, 50, 25, 10, 5, 2.5, and 1 °C/min) before the final crystallization temperature was reached (most commonly 10 °C). In some regimes the cooling rate was varied above and below an intermediate temperature of 130 °C. Specific thermal regimes are provided along with the corresponding data in the text. Samples were held overnight at 20 °C before being opened for study, or analyzed by differential scanning calorimetry.

Techniques. Samples for microscopy, DSC, and wide-angle X-ray diffraction (WAXD) were prepared using a Perkin-Elmer DSC 7 instrument, operated by Pyris software (Perkin-Elmer Instruments, Norwalk, CT). Thermal analysis of the samples was performed on a

Thermal Advantage Q100 DSC instrument using Thermal Advantage Universal Analysis software (TA Instruments, New Castle, DE). Two DSC instruments were used so that occasional pan explosions due to pressure buildup during preparation would not foul the furnace and affect the sensitivity of the DSC instrument used for analysis. Both optical and polarized light microscopy were performed on an Olympus BX41 microscope (Hitech Instruments, Edgemont, PA) equipped with a SPOT Insight QE camera, and analysis was completed using SPOT analytical and controlling software (SPOT Diagnostic Instruments, Sterling Heights, MI). An optical pressure cell, constructed from an HPLC UV–vis detector, was utilized in conjunction with a Linkam LTS 350 hot stage and LinkSys 32 temperature control and data acquisition software (Linkam Scientific Instruments, Surrey, U.K.) to visualize the processes of spherulite formation and dissolution. Average spherulite sizes were determined from a count of between 50 and 70 spherulites (all measurements made at 45° to the horizontal) from approximately four fields (40 \times).

WAXD data were collected in digital form using a Rigaku Geigerflex powder diffractometer with a Dmax-B controller and a vertical goniometer. Operation was in the θ – θ geometry. The instrument uses radiation from a copper target (Cu $K\alpha$ radiation, $\lambda = 1.54$ Å, including both the Cu $K\alpha_1$ and $K\alpha_2$, whereas Cu $K\beta$ was eliminated with a graphite monochromator). Samples were scanned continuously from $2\theta = 2^\circ$ to $2\theta = 30^\circ$ at a rate of 0.25 deg/min, and data were collected at intervals of 0.02°. WAXD samples were prepared by equilibrating starch/water mixtures on glass slides to constant water content at 20 °C and 85% relative humidity over potassium chloride (KCl) for 48 h. Percent crystallinity was approximated as the ratio of the resolved intensity of the crystalline reflection to the total integrated intensity.³⁶

Results and Discussion

Morphology. For a constant quench temperature of 10 °C, amylose formed spherulites at all cooling rates employed (Figure 2). For samples cooled directly from 180 to 10 °C, there was little change in mean spherulite size with cooling rate in the range 1–250 °C/min (Figure 3). Accuracy of cooling rates above 50 °C/min is tenuous, which may account for the lack of sensitivity to the rate above this value. Spherulites could also be formed from the parent maize starch at cooling rates exceeding 2.5 °C/min (Figure 3), but they exhibited a greater variation in average diameter as a function of cooling rate. We previously reported that for mung bean starch the mean spherulite diameter was reduced to the point of being immeasurable using light microscopy (<1 μm) at slow rates.²¹ Amylopectin did not form a spherulitic morphology at any of the cooling rates utilized in this study. Instead small nonbirefringent

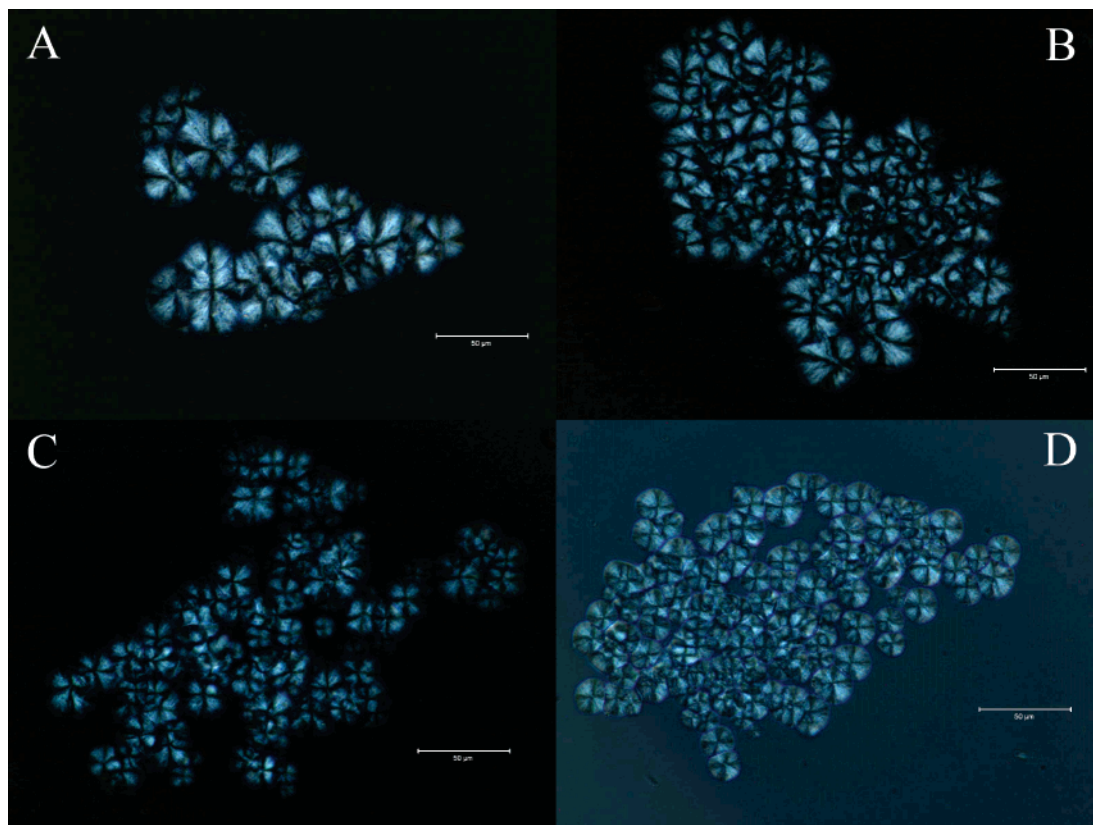


Figure 2. Representative optical micrographs showing birefringent spherulites formed from linear amylose cooled from 180 to 10 °C: A, sample cooled at 5 °C/min; B, cooled at 10 °C/min; C, cooled at 50 °C/min; D, cooled at 250 °C/min. Samples viewed between crossed polarizers. All scale bars equal 50 μm .

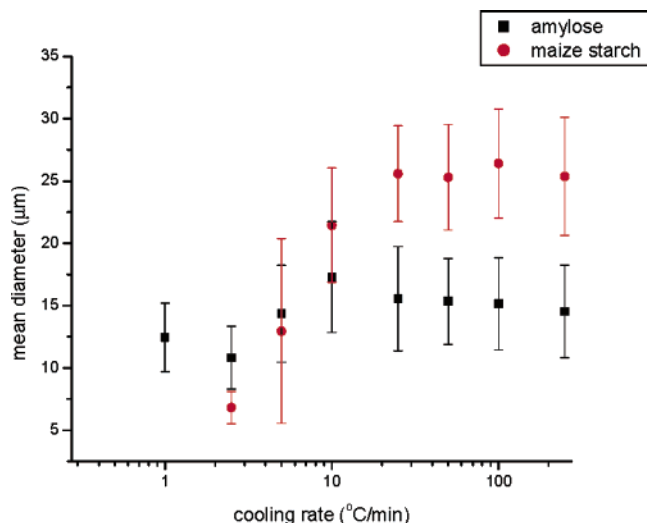


Figure 3. Dependence of average spherulite diameter vs cooling rate for linear amylose and maize starch cooled from 180 to 10 °C. Maize starch formed no discernible spherulitic material at 1 °C/min.

precipitates were formed, together with large transparent filmlike structures.³⁷

Although all processing conditions resulted in semicrystalline spherulitic structures, amylose samples cooled at slower rates formed fewer spherulites and an increasing amount of non-spherulitic material. The nonspherulitic precipitate exhibited little birefringence, and there were no additional thermal events detected by DSC. For common maize starch this nonspherulitic material was the only structure observed after cooling at 1 °C/min. We conclude that gel formation is likely under the conditions where spherulites do not form.^{38,39}

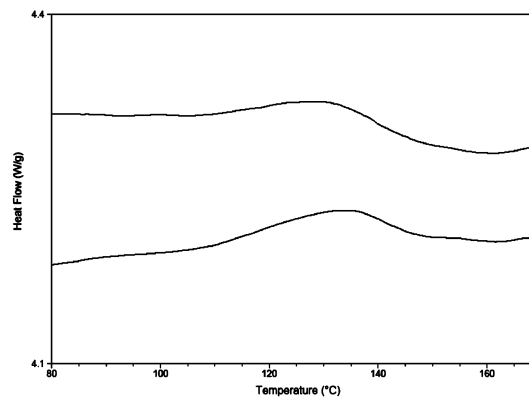


Figure 4. DSC thermograms on reheating (10 °C/min) for amylose cooled from 180 °C at 5 (bottom) and 10 (top) °C/min, endotherm up.

Characterization of Crystal Structure. The peak temperature or enthalpy of “melting” of spherulites, always observed as a very broad endotherm (Figure 4), does not change significantly in response to a change in cooling rate (Figure 5). Unlike mung bean starch, there were no multiple endotherms for samples prepared at slow cooling rates, which we previously proposed to be associated with the melting transition of a gel-like material’s crystalline junction zones, consistent with the visual observation of a large increase in the content of gel-like material formed at slow cooling rates.²¹ The relative lack of such material in amylose samples and the concurrent absence of the higher temperature endotherm are consistent with the near absence of gelation in amylose wherein spherulites form.⁴⁰ It is also possible that any gel-like material and the spherulites have the same melting point, as has been observed for isotactic polystyrene (iPS) in *cis*-decalin.⁴¹

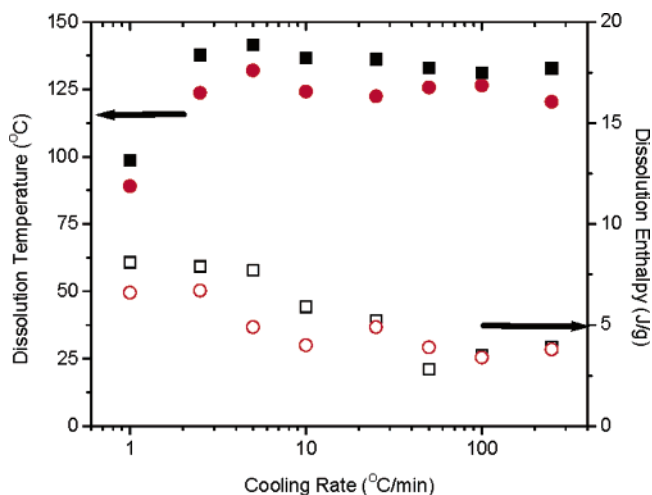


Figure 5. Effect of the cooling rate on the subsequent melting process during heating of spherulitic amylose: □, 20% starch solution; ○, 10% starch solution. Hollow symbols represent dissolution enthalpy (± 2 J/g) and solid symbols represent the dissolution temperature (± 5 °C, due to the rather broad and shallow transitions) for the starch solution.

The calorimetric response includes both the melting of crystalline starch and the hydration of the polymer. Due to favorable amylose–water interactions, it has been postulated that low transition enthalpies should be observed, even at higher degrees of crystallinity.⁴² Utilizing a pressure cell and the same heating rate as in our DSC experiments (10 °C/min), melting was visually observed as a loss of birefringence and the complete disappearance of spherulites over the range of temperatures corresponding to the DSC endotherm. Increasing the amylose concentration from 10% to 20% (w/w) had the effect of raising the peak temperature by an average of about 10 °C. The spherulite size was essentially unchanged at the higher starch concentration.

The average enthalpy decreased for both concentrations as the rate of cooling was increased from 1 to 50 °C/min (Figure 5), but the range of values is small. The observed melting temperatures approach the extrapolated “dissolution” temperature for linear dextrin of infinite molecular weight—147 °C—where the volume fraction of water was 0.8.⁴³ The temperatures reported in Figure 5 are higher than those observed for mung bean starch prepared under the same conditions,²¹ in keeping with the greater linearity of the leached amylose and higher overall amylose content.

B-type crystallinity (as evidenced by WAXD peaks at approximately $2\theta = 5^\circ, 17^\circ, 23^\circ,$ and 25°) was observed for all samples (Figure 6), as expected given the high degree of hydration for the samples under investigation here.^{44–46} The absence of reflections characteristic of the V-type crystal structure confirmed that lipid complexes are not responsible for the crystallinity.⁴⁷ The relative degree of crystallinity estimated from the WAXD patterns was $\sim 20\%$, independent of the cooling rate between 5 and 250 °C/min.

Crystallization Temperature. Amylose solutions were quenched from 180 °C at 250 °C/min to a variety of crystallization temperatures (T_c) in the range 20–120 °C to determine the temperature range over which a spherulitic morphology develops. Samples were held at the crystallization temperature for 24 h, the pans opened, and the morphology was immediately viewed. Well-formed spherulites were observed at T_c values of 60 °C and below (Figure 7A), while a transitional morphology of poorly formed spherulites was seen at 70 °C (Figure 7B). Of note is that the onset of solvent-facilitated dissolution of

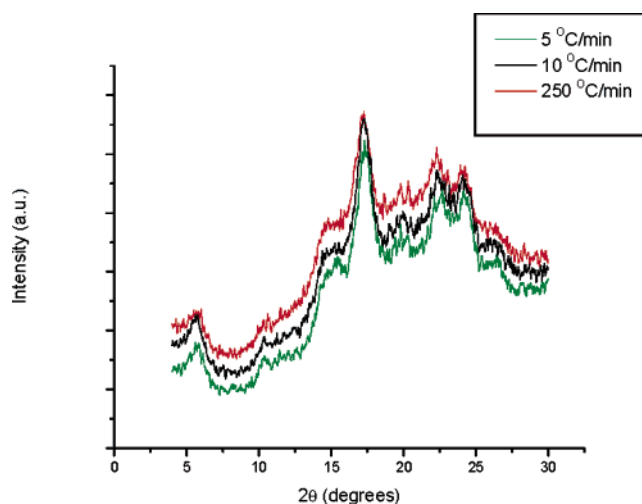


Figure 6. WAXD patterns for starch spherulites from a 20% (w/w) linear starch dispersion cooled from 180 °C at 5 (bottom), 10 (middle), and 250 (top) °C/min. The WAXD samples were equilibrated at 20 °C and 85% humidity for 48 h prior to analysis.

crystalline amylose has been placed at about 70 °C.⁴² Above 70 °C the spherulitic morphology disappeared and was replaced by a “salt-and-pepper”-like morphology with some large feather-like crystalline structures. At the highest T_c values (110 and 120 °C) small spherulites were seen to form from an initially clear solution as the specimen cooled to ambient temperature on the microscope slide. Spherulite sizes increased with increasing hold temperature between 20 and 70 °C. The initial increase in spherulite size with increasing T_c , followed by a transition to a nonspherulitic morphology, is consistent with our previous observations for mung bean starch.²¹

Cooling Rate Variation. Amylose is thought to complete solvent-facilitated dissolution at about 130 °C.³⁸ Therefore, aqueous amylose solutions were quenched from 180 to 130 °C (at 250 °C/min), from which the system was subsequently slowly cooled (at 1 and 2.5 °C/min) to 10 °C. It was hypothesized that gel formation would be avoided by the rapid quench to 130 °C, and that the spherulite size would increase at slower cooling rates below 130 °C. Substantially more spherulitic, and much less gel-like, material was observed for samples quickly cooled to 130 °C, compared to those cooled directly from 180 to 10 °C at the same rate (Figure 8). There was a large increase in the size of the birefringent structures for samples that were quickly cooled from the highest temperatures, as seen in the comparison of part A to part B and part C to part D of Figure 8. The initiation of gelation at higher temperatures in samples slowly cooled directly from 180 °C would restrict the size and number of spherulites in Figure 8A,C. As expected, smaller, more numerous, and better formed spherulites were observed in samples cooled more rapidly below 130 °C (compare Figure 8B to Figure 8D). Relatively small spherulites were observed in samples very rapidly quenched from intermediate temperatures (110–130 °C) to room temperature (20 °C) on the microscope slide (see, for example, Figure 7E), suggesting that little aggregation (preordering) had occurred during the 24 h holding period at these temperatures prior to observation.

Discussion. It is apparent from this study that the more linear fraction of starch readily forms spherulites. However, we are left with several vexing questions.

Why Is It Necessary To Heat Starch to a Temperature > 170 °C To Form Spherulites on Cooling? We previously reported that it was necessary to heat most starches above 170 °C to form a spherulitic morphology on cooling, and suggested that

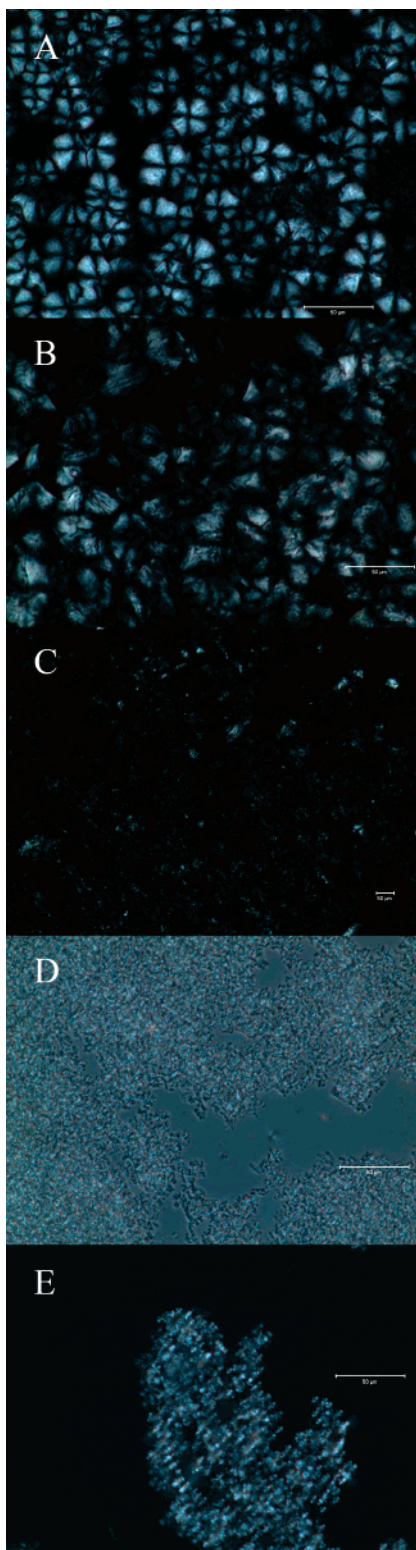


Figure 7. Morphology of amylose samples held at 40 (A), 70 (B), 90 (C), 100 (D), and 110 (E) °C for 24 h, after heating to 180 °C and cooling at the maximum rate of 250 °C/min. All scale bars equal 50 μm.

this may be related to changes in chain stiffness at high temperature.²⁰ A reviewer of a previous paper had suggested that heating to high temperature degraded the starch to short-chain amyloextrins ($dp < 25$), so that what we observed was merely equivalent to that reported by Ring et al.⁴⁸ for low molecular weight amylose. Amylose was heated to 180 °C in the DSC instrument as described in the Experimental Section

and cooled at 10 °C/min to 10 °C and the resulting starch polymer then characterized using intrinsic viscosity. The calculated degree of polymerization was 635, or about 30% below the starting value of 925. This demonstrated that short-chain amyloextrins are not solely responsible for the formation of the spherulites, since this was the only morphology observed.

We reasoned²⁰ by analogy to iPS in *cis*-decahydronaphthalene and aqueous agarose solutions that a helix \rightarrow coil transition occurred at 170 °C, increasing chain flexibility and permitting chain folding, as was assumed to occur in spherulites.⁴⁹ While we now question the chain folding aspect of this hypothesis (see below), we still believe a helix \rightarrow coil transition occurs and that this transition is necessary for spherulite development, though for different reasons. *We hypothesize that, to obtain a spherulitic morphology on rapid cooling of native amylose, it is necessary to heat starch above a liquid crystal–isotropic phase boundary that coincides with a helix \rightarrow coil transition, to remove helical nuclei that otherwise would cause gel formation on cooling.*

It has long been known that amylose “solutions” must be heated to about 170 °C to obtain optical clarity.^{50,51} We have also observed such a phenomenon whether heating granular starches or redissolving precipitated amylose; i.e., the suspension remains turbid above the gelatinization/dissolution endotherm observed by DSC, only to clear at some higher temperature, usually greater than 170 °C. This very type of observation led to Reinitzer’s “discovery” of liquid crystals,¹⁴ and the characteristic temperature at which the liquid crystal phase becomes isotropic is called the “clearing temperature”.¹³

Polymer liquid crystals are favored by conformations that alternate between rigid segments and more flexible regions. Banks and Greenwood⁵² concluded that amylose was a random coil containing short helical segments with a Kuhn statistical segment derived from viscosity data of 21 Å in aqueous 0.33 M KCl. Nikuni⁵³ called amylose a “random helical chain” and even built models out of a metal chain (see, for example, Figure 17 in ref 53).

Gidley⁵⁰ refers to amylose solutions as “inherently unstable”, and while Ring et al.⁵⁴ claimed to have prepared “true molecular solutions” free of retrograded amylose by aqueous leaching between 62 and 80 °C, extensive precipitation was observed at times > 12 h. LeLay and Delmas used the term dissolution to indicate the loss of “melttable order” generally measured by DSC, but concluded it does not signify that the amylose–water mixture is in a “real” solution.⁵¹ They observed a total enthalpy of disordering far in excess of the enthalpy of gelatinization (60 J/g vs 16 J/g), and concluded that the excess enthalpy must correspond to the transformation of single helices into random coils.⁵¹ Using Fourier transform IR spectroscopy, van Soest et al.⁵⁵ observed the loss of “short-range order” in native potato starch containing 26% water (w/w) over the temperature range 110–195 °C, with 13% still present at 170 °C, vanishing by 195 °C, close to the melting temperature of glucose (190 °C).⁴²

Loss of molecular order, associated with the double-helix content, and crystalline order are thought to occur simultaneously on melting; Cooke and Gidley⁵⁶ concluded that the enthalpy of starch gelatinization primarily reflected loss of double-helical order vis-à-vis crystal packing. This was confirmed by Waigh et al. for waxy maize starch.⁵⁷ However, for amylose, Bernazzani et al. disagree.⁴² They showed by DSC and IR that “double helices” persisted beyond the loss of crystallinity as determined by X-ray diffraction, with an increasing content of single helices in the range 50–120 °C, but concluded that a loss of double-helical order does not lead

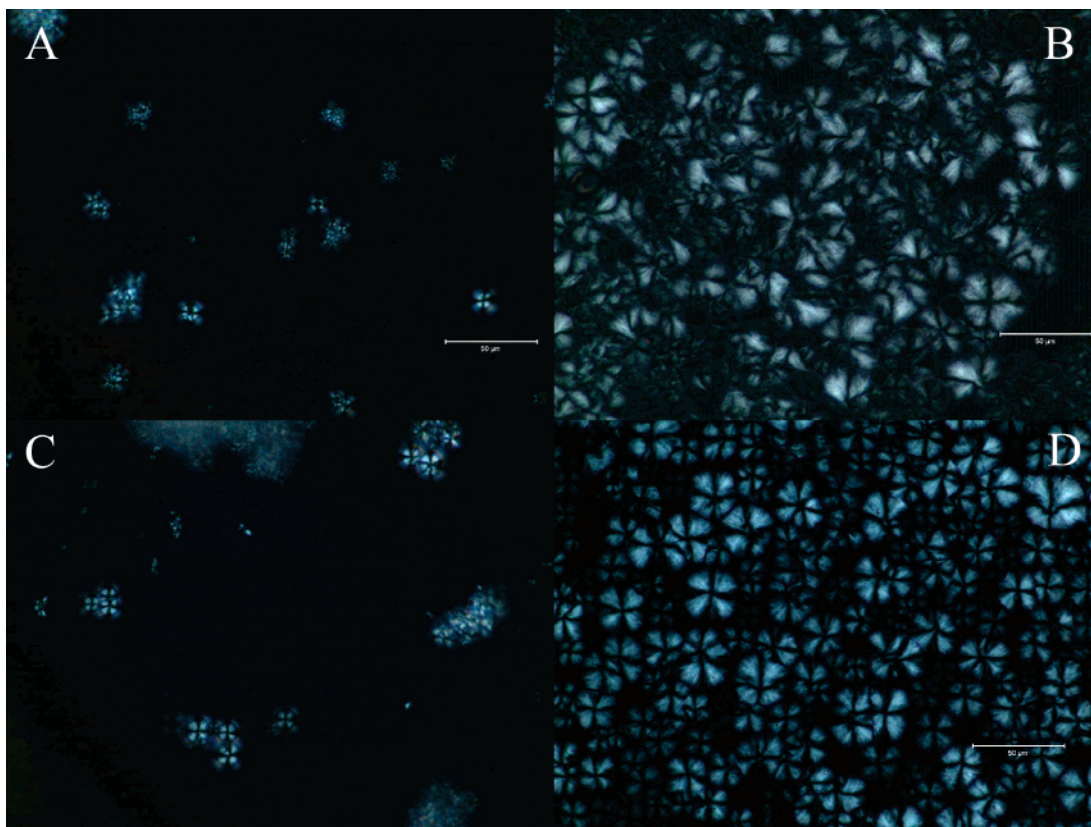


Figure 8. Representative optical micrographs depicting the change in morphology for linear starch cooled rapidly to an intermediate temperature, followed by slow cooling vs simply slow cooling: A, amylose cooled at 1 °C/min from 180 to 10 °C; B, cooled from 180 to 130 °C at 250 °C/min, followed by cooling at 1 °C/min to 10 °C; C, cooled at 2.5 °C/min from 180 to 10 °C; D, cooled from 180 to 130 °C at 250 °C/min, followed by cooling at 2.5 °C/min to 10 °C. All micrographs were acquired at the same magnification. Scale bars equal 50 μm .

after melting to a single-helix conformation. However, the loss of molecular order on heating has been associated with the transformation of double helices into single helices,⁵⁸ and they themselves⁴² demonstrated a “clear inverse correlation” between IR bands associated with single and double helices. In a later paper, these authors⁵⁹ suggested that the observed changes in the IR spectra between 70 and 105 °C could correspond to a transformation of a network of double helices into freer chains, possibly single helices. Moreover, Gidley saw no change in the optical rotation on gelation of amylose and concluded that the “true optical rotation” of the ordered double helix is very similar to the value observed [in solution at <160 °C].⁵⁰ Identical C-1 chemical shifts for amylose solutions and solid B-type amylose implied that the double-helical conformation was similar to the weighted average solution conformation.⁵⁰ The reverse would also be true, i.e., that the weighted average conformation in solution at <160 °C is similar to that of solid B-type amylose. For B-type starches, the DSC endotherm occurs well before the final loss of helices, showing an increased contribution of a smectic/nematic \rightarrow isotropic transition followed by helix unwinding.⁵⁷

Explanations for the effect of chain length on the kinetics of amylose aggregation invoke the presence of regions of helical conformation within the chains, but Gidley and Bulpin³⁵ concluded that there was no convincing experimental evidence for this assertion and that the relatively short persistence length (12.1 Å) would seem to preclude significant helical segments. However, a persistence length of 27.8 Å in water at room temperature was reported by Ring et al.,⁵⁴ in excess of the minimum needed for helix formation.⁶⁰ Bayer and Baltá Calleja⁶¹ calculated a persistence length of 28.7 Å for amylose, presumably in water at room temperature, equivalent to 1.12

turns of the single helix. They suggested that, due to the high flexibility of the single helix, amorphous amylose may exist as single helices in a statistical random conformation. Once formed, small helices may be stabilized by the “induced rigidity effect” to higher temperatures in the nematic state by their neighbors.⁵⁷ Individual amylose chains have been visualized using AFM.^{62,63} Noncontact AFM images show synthetic amylose to be single chains of pseudohelical conformation when dissolved in water at 90 °C.⁶³ Furthermore, there appears to be a favored orientation of the molecules on the mica surface, but it is not known to what degree the surface acts as a template. A similar favored orientation of helical segments was visible in AFM images of amylose/iodine/lipid complexes.⁶² The length of the apparently stiff, straight segments is several hundred nanometers in both cases;^{62,63} combined with a thickness of 0.54 nm,⁶³ this yields an aspect ratio in the range 250–500 very similar to that of xanthan, which is known to form anisotropic mesophases.¹ Theories of flexible-chain polymers show that the rigidity induced by a coil \rightarrow helix transition could provide the necessary stiffness for liquid crystal formation.¹⁵

Figure 9 is a conceptual model for the behavior of concentrated amylose–water mixtures on heating. Double-helical crystallites “melt” (or “dissolve”) on heating at about 70 °C, and fixed network entanglements are thermally dissociated by 130 °C^{42,51,59,61} to form a liquid crystalline phase (probably nematic as most lyotropic LCs¹³) comprising relatively flexible chains with some regions of rigid helical conformation. These regions are stabilized by near neighbors. On heating, both the number and length of these regions decreases, and the system becomes isotropic at a temperature between 160 and 180 °C. The polymer–solvent interaction parameter, χ , is approximately 0.8 for amylose in water at room temperature, but falls to 0.5

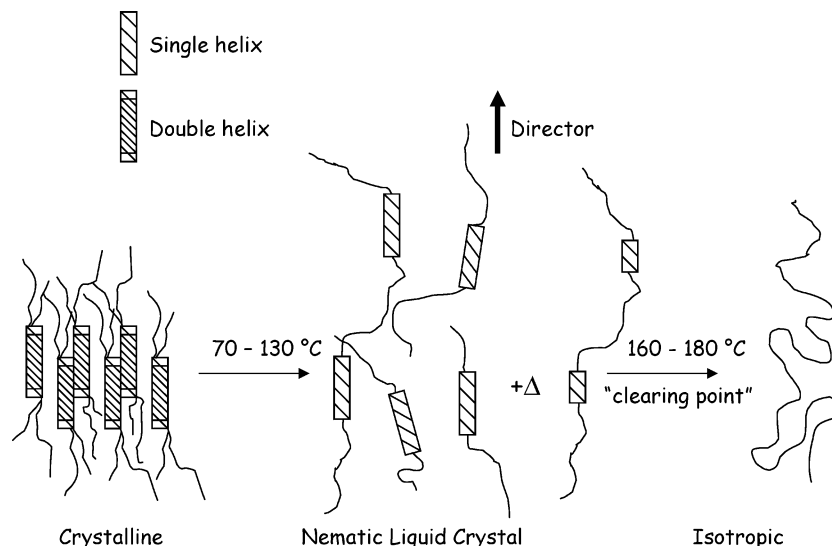


Figure 9. Schematic of proposed transitions on heating crystalline amylose in excess water. In addition to crystallite melting/dissolution between 70 and 130 °C, relaxation of fixed network entanglements also occurs. See the text for details.

between 160 and 180 °C.⁴³ Benczédi et al. report a transition to Flory sorption at 175 °C for the starch–water system,⁶⁴ implying that remaining starch–starch hydrogen bonds are replaced by starch–water hydrogen bonds above this temperature. They state further that the ability of starch to recrystallize partially is only lost at these high temperatures in a transition involving the breakage of intramolecular hydrogen bonds.⁶⁵

This “thermotropicity” in a lyotropic liquid crystal of κ -carrageenan was explained on the basis of either a temperature dependence of the persistence length or the gradual shift of the helix \leftrightarrow coil equilibrium toward the coiled state at higher temperature.⁶⁶ For κ -carrageenan, biphasic behavior has been observed up to about 60 °C, after which no texture was observed, the solution was macroscopically isotropic when viewed between crossed polarizers, and the characteristic correlation peak in SAXS had disappeared.⁶⁶ The investigators concluded that a helix \rightarrow coil transition was responsible for the disappearance of anisotropy at 65 °C. Likewise, xanthan gum forms an anisotropic mesophase that disappears above temperatures characteristic of a helix \rightarrow coil transition.¹ Like Borgström et al.,⁶⁶ we have assumed that the single helix is the nematogenic structure, but cannot rule out superhelical aggregates as such. Sequences with up to 14 monomers in a 3_1 helical conformation are responsible for the smectic layering in isotactic polypropylene (iPP).¹⁵

This is not the first time a liquid crystal model has been proposed for starch. Waigh et al. proposed a chiral side-chain liquid crystal model for amylopectin that transitioned through smectic \rightarrow nematic \rightarrow isotropic phases on heating under limited water conditions.⁶⁷ They concluded from ¹³C CP/MAS NMR evidence that a “true” helix \rightarrow coil transition occurred above 69 °C (the end point of gelatinization), but it is unclear from their diagrams (see, e.g., Figures 8 and 10 in ref 67) whether they believed in a simple transition from double helices to a completely random coil conformation, or to the assumed solution conformation that may include single helices. We propose a main-chain lyotropic liquid crystalline model for concentrated amylose–water systems between about 130 and 170 °C, the actual temperatures depending on numerous factors including amylose chain length. We suggest that spherulites form in the anisotropic phase of a biphasic system. It is the presence of the isotropic solution that is prerequisite for spherulite formation on cooling.

One lingering question is whether double helices can simply untwist to form single helices or it is necessary to proceed through a random coil conformation. The fact that there is no clear exotherm between the melting of double-helical, crystalline starch and the appearance of the V_h single-helical polymorph on heating⁶⁸ suggests that a direct double-helix to single-helix transformation can take place. Double helices can be shown⁶¹ to arise from the bare rapprochement of single helices provided the single helices contain band-flip motifs.⁶⁹

What Happens on Cooling and What is the Nature of the “Memory Effect” in Solutions Heated to <170 °C? The phenomenon whereby athermal nucleation is observed in a cooled melt after heating above the melting temperature is referred to as a memory effect. This behavior is illustrated by agarose, where heating of aqueous gels to 100 °C does not produce the same results as heating to 130 °C prior to cooling. Gels “melted” at 100 °C contained aggregates as evidenced by small-angle neutron scattering⁷⁰ that were considered possible nematic-like mesophases such as those observed in sPMMA/chlorobenzene between 35 and 55% (w/w), which is helicoidal above the gel melting temperature.⁷¹ Agarose exists as a loose helix with a 9–12 nm persistence length in the sol state.⁷² The tendency of helices to associate increases with decreasing charge density, so neutral agarose shows extensive association,⁷³ and one could expect the same of amylose. Liquid crystalline phases are more stable than crystals, so melting of crystals does not lead to a homogeneous fluid, but one containing domains that can serve as nuclei on cooling.¹⁵

We proposed that spherulite formation should be considered in light of a competition between phase separation and crystallization (gelation).²¹ Spherulites form only if one can induce phase separation well in advance of crystallization by rapidly quenching the system from the isotropic state into a two-phase region. Otherwise, preformed nuclei initiate crystallization, i.e., gel formation, too rapidly. The gel thus formed prevents further phase separation.⁷⁴ We described²¹ the situation through a phase diagram that, in light of the preceding discussion, must be refined.

The phase diagram included a miscibility gap, the position of which was cooling rate dependent, well below the equilibrium liquidus curve. When rapidly quenched into the miscibility gap, amylose solutions would demix prior to crystallization, forming two phases, one polymer-poor and the other polymer-rich. The

concentration of these phases is dependent only on the quench temperature; hence, once crystallization occurs, one expects a nonvariant melting point.⁷⁵ We hypothesized that spherulites form in the polymer-rich phase.²¹ Consistent with our hypothesis, Gidley and Bulpin³⁵ observed the development of turbidity in clear solutions of amylose (heated to 160–170 °C for 10–20 min) to be highly cooling rate dependent, occurring up to 35 °C lower at 1 °C/min vs 0.15 °C/min, and Miles et al. concluded that the local composition of the polymer-rich phase in amylose gels was independent of overall polymer concentration.²³ However, should crystallization be preceeded with existing nuclei, such as remnants of liquid crystalline phases, so that it occurs prior to or coincident with macroscopic phase separation, gelation would be favored. Samples of iPP containing liquid crystalline phases showed faster crystallization kinetics than samples without; smectic phases induced epitaxial growth of crystals, but did not crystallize themselves.¹⁵ Gelation can also hinder the further development of liquid crystalline order, as in the case of κ -carrageenan.⁶⁶

Solutions of amylose enter a metastable state below 80 °C.⁷⁶ Divergent clustering functions observed below 80 °C reflect a tendency of water to phase separate from starch. This coincides closely with the quench temperature required to form spherulites from amylose (Figure 7) or mung bean starch.²¹ When held just above this temperature for 24 h, amylose solutions became birefringent but not spherulitic (Figure 7C). In previous work, mung bean starch produced large birefringent “sheets” that could be interpreted as a Schlieren texture characteristic of liquid crystals (see Figure 8H of ref 21).

The preceding argument explains the “surprising results” of Doublier et al.,³⁸ where a gel formed on cooling if amylose was dissolved at temperatures below 160 °C, while amylose crystals precipitated out of solutions heated at higher temperatures. The rate of turbidity development depended on the concentration and dissolution temperature (T_d). The higher the T_d , the slower the development of turbidity; e.g., cloudiness appeared only after 30 min for $T_d = 172$ °C. Unlike amylose gels, “precipitates” displayed exceptionally sharp WAXD diffraction patterns. Doublier et al.³⁸ give an explanation much like the one we advance above, with the exception of not identifying the “nuclei in the solution” with a liquid crystalline phase and the precipitates as spherulites.

Other data should be revisited in light of this proposed mechanism. For example, Vesterinen et al. demonstrated a maximum in rigidity as a function of dissolution temperature for gels from high-amylose starch, occurring between 150 and 155 °C, which they attributed to polymer degradation above this temperature.⁷⁷ However, amylose is apparently stable at 160–170 °C for 10–20 min.⁶⁰ When heated above the optimum temperature (152 °C), they⁷⁷ showed a longer induction time and slower rate of growth in rigidity that paralleled the turbidity results of Doublier et al.³⁸ We suggest that this maximum in rigidity represents an optimal balance between solubilization of the starch and retention of nuclei.

Why Is There Hysteresis between Dissolution and Crystallization? Once heated above the liquid crystal–isotropic phase boundary, κ -carrageenan liquid crystals regained their structure only very slowly (matter of days).⁶⁶ This was not due to a reorientation of domains, but to the recovery of “local” structure. Hysteresis between dissolution and nucleation has also been observed for DNA crystallization,⁶ and is a well-established behavior of synthetic polymers explained by the Hoffman–Lauritzen kinetic model of polymer crystallization.⁷⁸ We think it likely that nucleation of single helices of sufficient length

and appropriate conformation (perhaps band-flip motifs)^{61,69} within the amylose chain is a significant kinetic barrier to crystallization.

What Is the Nature of the Crystallinity in the Spherulite Relative to the Chain Conformation (i.e., Chain Folded or Fringed Micelle)? It is often assumed that polymer spherulites are spherically symmetric arrays of chain-folded lamellae.^{28,49,79,80} Monar and Phillips⁶ concluded that DNA forms helical chain-folded lamellae when crystallized as spherulites. However, the intrinsic chain stiffness of most polysaccharides does not allow chain folding within a confined volume.¹ Guenet employs this argument to conclude that intrinsically rigid agarose chains cannot chain fold and hence cannot produce spherulites but only gels.⁴⁹ Sakamoto et al.⁸ concluded that the extended-chain crystal was more plausible than a chain-folded one for single crystals of α -chitin. However, the amylose helix is more flexible than agarose or chitin. AFM images of amylose with single-helical segments induced by iodine and lipid complexes unequivocally demonstrate the ability of amylose to chain fold.⁶² Even so, Bayer and Baltá Calleja found it unreasonable to assume that immobile double helices could chain fold, and that the crystalline structure of amylose probably corresponds more closely to a fringed micelle.⁶¹

Both the A and B crystalline allomorphs of starch are thought to be composed of assemblies of left-handed, parallel-stranded double helices.^{81,82} The simplest model of chain folding to form double helices would result in antiparallel alignment of the two chains. However, parallel chain alignment could easily be accommodated by a fringed micelle model.

Cholesteric liquid crystal “germs” with the appearance of banded negatively birefringent spherulites have been observed in 5% (w/v) of DNA.⁵ At 25% (w/v) crystalline spherulites were formed that differed from these cholesteric germs by the absence of banding. Banded cholesteric and crystalline spherulites appeared in aqueous solutions of collagen-like peptides at concentrations >20 mg/mL.¹¹ While we propose the presence of lyotropic liquid crystalline phases in amylose–water mixtures, we assume that the spherulites formed are truly crystalline at temperatures below 70 °C. However, liquid crystalline preordering may influence the final crystalline morphology. Li and de Jeu¹⁵ show smectic-bundle-induced crystallization of iPP that results in “transcrystallites”. These transcrystallites are nearly identical to what we referred to as “row-nucleated” structures (see, for example, Figure 4 in ref 21 or Figure 2A in ref 20). They concluded that smectic bundles favor fringed-micelle nuclei.

The amylose spherulites observed here were negatively birefringent, implying that the main chain axes were tangential to the radius of the spherulite. While it is straightforward to visualize a chain-folded lamella growing radially that would result in such an orientation, it is less obvious why lamellae comprising fringed micelles should be so oriented.

If Spherulite Formation Requires Heating to 170 °C, How Can It Possibly Be Involved in Granule Initiation? In a previous paper²¹ we argued that spherulite formation could serve as a model for granule initiation in vivo. In part, this was based on the chemical and physical similarities between spherulites and the core or hilum region of starch granules. We speculated that the structure of α -glucans formed early in starch synthesis is suited to spherulite formation, and that during synthesis they exist as random coils and are stable in this conformation, and hence do not aggregate for a time period long enough so that a sufficient concentration for phase separation builds up in the amyloplast. Ring et al.⁵⁴ stated that leached amylose is stable

in solution for several hours. Once phase separation occurs and a polymer-rich phase is created, crystallization in spherulitic morphology is rapid.

Concluding Remarks

Predictions can now be made about the tendency of a starch–water system to form a particular morphology, based both on the composition of the starch (ratio of amylose to amylopectin) and on the processing conditions. Within these factors, maximum heating temperature, cooling rate, quench temperature, and amylose content play major roles in determining the final morphology.

The formation of spherulites from amylose solutions occurred over a wide range of cooling rates and quench temperatures. The ability of native starches to form spherulites is highly variable,²⁰ and this is likely due to the ratio of amylose to amylopectin as well as differences in the molecular architecture of the starch polymers. Differences in the solubility of amylose and amylopectin are well-known,⁸³ and these differences may play a prominent role in determining the liquid–liquid demixing behavior that we conjecture plays a crucial role in the formation of the spherulitic morphology. Indeed, it has been previously recognized that amylopectin can hinder phase separation in starch containing both polymers.⁷⁶

Confirmation or refutation of the foregoing ideas awaits further investigation employing techniques sensitive to chain conformation, e.g., SAXS, CD, FTIR, or NMR. The challenge to investigating the starch–water system with these techniques is in working at high temperature with a volatile solvent. Further investigation should include the influence of the amylose chain length and concentration of morphology.

Acknowledgment. We express our appreciation to the USDA-NRICGP program for support for this research. We thank Dr. Alan Benesi for assistance with the NMR. We also thank Jesse Qian and Farai Machina for their assistance.

References and Notes

- Lapasin, R.; Prici, S. *Rheology of Industrial Polysaccharides: Theory and Applications*; Blackie Academic and Professional: London, 1995; pp 1–133
- Rill, R. L. *Proc. Natl. Acad. Sci. U.S.A.* **1986**, *83*, 342.
- Davidson, M. W.; Strzelecka, T. E.; Rill, R. L. *Nature* **1998**, *331*, 457.
- Monar, K.; Phillips, P. J. *J. Polym. Sci., Part B: Polym. Phys.* **1997**, *35*, 1843.
- Zakharova, S. S.; Jesse, W.; Backendorf, C.; van der Maarel, R. C. *Biophys. J.* **2002**, *83*, 1119.
- Monar, K.; Phillips, P. J. *Macromolecules* **1999**, *32*, 5852.
- Murray, S. B.; Neville, S. C. *Int. J. Biol. Macromol.* **1997**, *20*, 123.
- Sakamoto, J.; Sugiyama, J.; Kimura, S.; Imai, T.; Itoh, T.; Watanabe, T.; Kobayashi, S. *Macromolecules* **2000**, *33*, 4155.
- Murray, S. B.; Neville, S. C. *Int. J. Biol. Macromol.* **1998**, *22*, 137.
- Tanaka, T.; Magoshi, J.; Magoshi, Y.; Lotz, B.; Inoue, S–I.; Kobayashi, M.; Tsuda, H.; Becker, M. A.; Han, Zh.; Nakamura, Sh. *J. Therm. Anal. Calorim.* **2001**, *64*, 645.
- Martin, R.; Waldmann, L.; Kaplan, D. L. *Biopolymers* **2003**, *70*, 435.
- Krebs, M. R. H.; MacPhee, C. E.; Miller, A. F.; Dunlop, I. E.; Dobson, C. M.; Donald, A. M. *Proc. Natl. Acad. Sci. U.S.A.* **2004**, *101*, 14420.
- Sperling, L. H. *Introduction to Physical Polymer Science*, 2nd ed.; John Wiley & Sons: New York, 1992; pp 279–302.
- Collins, P. J. *Liquid Crystals: Nature's Delicate Phase of Matter*, 2nd ed.; Princeton University Press: Princeton, NJ, 2002; p 20.
- Li, L.; de Jeu, W. H. *Faraday Discuss.* **2005**, *128*, 299.
- Smith, A. M. *Biomacromolecules* **2001**, *2*, 335.
- Berghmans, H.; Aerts, L.; Buyse, K.; Deberdt, F.; Roels, T.; De Rudder, J.; Vereecke, S. *Ber. Bunsen-Ges. Phys. Chem.* **1998**, *102*, 1654.
- Nordmark, T. S.; Ziegler, G. R. *Carbohydr. Polym.* **2002**, *49*, 439.
- Nordmark, T. S.; Ziegler, G. R. *Carbohydr. Res.* **2002**, *337*, 1467.
- Ziegler, G. R.; Nordmark, T. S.; Woodling, S. E. *Food Hydrocolloids* **2003**, *17*, 487.
- Ziegler, G. R.; Creek, J. A.; Runt, J. *Biomacromolecules* **2005**, *6*, 1547.
- Cheetham, N. W. H.; Tao, L. *Carbohydr. Polym.* **1998**, *36*, 277.
- Miles, M. J.; Morris, V. J.; Ring, S. G. *Carbohydr. Res.* **1985**, *135*, 257.
- Rindlav-Westling, A.; Stading, M.; Gatenholm, P. *Biomacromolecules* **2002**, *3*, 84.
- Phillips, P. J. In *Handbook of Crystal Growth 2. Bulk Crystal Growth. Part B: Growth Mechanisms and Dynamics*; Hurler, D. T. J., Ed.; North-Holland: New York, 1994; p 1167.
- Chowdhury, F.; Haigh, J. A.; Mandelkern, L.; Alamo, R. G. *Polym. Bull.* **1998**, *41*, 463.
- Whittam, M. A.; Noel, T. R.; Ring, S. G. *Int. J. Biol. Macromol.* **1990**, *12*, 359.
- Bassett, D. C.; Oiley, R. H.; Sutton, S. J.; Vaughan, A. S. *Macromolecules* **1996**, *29*, 1852.
- Mua, J. P.; Jackson, D. S. *Cereal Chem.* **1995**, *78*, 508.
- Falk, H.; Micura, R.; Stanek, M.; Wutka, R. *Stärke/Starch* **1996**, *48*, 344.
- Stanek, M.; Falk, H.; Huber, A. *Monatsh. Chem.* **1998**, *129*, 355.
- Benesi, A. J.; Brant, D. A. *Macromolecules* **1985**, *18*, 1109.
- Banks, W.; Greenwood, C. T. *Carbohydr. Res.* **1968**, *7*, 414.
- Everett, W. W.; Foster, J. F. *J. Am. Chem. Soc.* **1959**, *81*, 3464.
- Gidley, M. J.; Bulpin, P. V. *Macromolecules* **1989**, *22*, 341.
- Hermans, P. H.; Weidinger, A. *J. Appl. Phys.* **1948**, *19*, 491.
- Creek, J. A.; Ziegler, G. R.; Runt, J. *Prog. Food Biopolym. Res.*, submitted for publication.
- Doublier, J. L.; Cote, I.; Llamas, G.; Charlet, G. *Prog. Colloid Polym. Sci.* **1992**, *90*, 61.
- Daniel, C.; Dammer, C.; Guenet, J-M. *Polymer* **1994**, *35*, 4243.
- Keller, A. *Faraday Discuss.* **1995**, *101*, 1.
- Klein, M.; Mathis, A.; Menelle, A.; Guenet, J-M. *Macromolecules* **1990**, *23*, 4591.
- Bernazzani, P.; Chapados, C.; Delmas, G. *J. Polym. Sci., Part B: Polym. Phys.* **2000**, *38*, 1662.
- Moates, G. K.; Noel, T. R.; Parker, R.; Ring, S. G. *Carbohydr. Res.* **1997**, *298*, 327.
- Wu, H–C. H.; Sarko, A. *Carbohydr. Res.* **1978**, *61*, 7.
- Waigh, T. A.; Hopkinson, I.; Donald, A. M.; Butler, M. F.; Heidebach, F.; Riekel, C. *Macromolecules* **1997**, *30*, 3813.
- Imberty, A.; Buleon, A.; Tran, V.; Perez, S. *Stärke/Starch* **1991**, *43*, 375.
- Buleon, A.; Colonna, P.; Planchot, V.; Ball, S. *Int. J. Biol. Macromol.* **1998**, *23*, 85.
- Ring, S. G.; Miles, M. J.; Morris, V. J.; Turner, R.; Colonna, P. *Int. J. Biol. Macromol.* **1987**, *9*, 158.
- Guenet, J-M. *Trends Polym. Sci.* **1996**, *4*, 6.
- Gidley, M. J. *Macromolecules* **1989**, *22*, 351.
- LeLay, P.; Delmas, G. *Carbohydr. Polym.* **1998**, *37*, 49.
- Banks, W.; Greenwood, C. T. *Stärke* **1963**, *15*, 166.
- Nikuni, Z. *Stärke/Starch* **1978**, *30* (4), 105.
- Ring, S. G.; l'Anson, K. J.; Morris, V. J. *Macromolecules* **1985**, *18*, 182.
- van Soest, J. J. G.; Tournois, H.; de Wit, D.; Vliegthart, J. F. G. *Carbohydr. Res.* **1995**, *279*, 201.
- Cooke, D.; Gidley, M. J. *Carbohydr. Res.* **1992**, *227*, 103.
- Waigh, T. A.; Gidley, M. J.; Komanshek, B. U.; Donald, A. M. *Carbohydr. Res.* **2000**, *328*, 165.
- Godet, M. C.; Tran, V.; Delage, M. M.; Buleon, A. *Int. J. Biol. Macromol.* **1993**, *15*, 11.
- Bernazzani, P.; Chapados, C.; Delmas, G. *Biopolymers* **2001**, *58*, 305–318.
- Gidley, M. J.; Bulpin, P. V. *Carbohydr. Res.* **1987**, *161*, 291.
- Bayer, R. K.; Balta Calleja, F. J. *J. Macromol. Sci., Phys.* **2005**, *44*, 479.
- Gunning, A. P.; Giardina, T. P.; Faulds, C. B.; Juge, N.; Ring, S. G.; Williamson, G.; Morris, V. J. *Carbohydr. Polym.* **2003**, *51*, 177.
- McIntire, T. M.; Brant, D. A. *Int. J. Biol. Macromol.* **1993**, *26*, 303.
- Benczedi, D.; Tomka, I.; Escher, F. *Macromolecules* **1998**, *31*, 3062.
- Benczedi, D.; Tomka, I.; Escher, F. *Macromolecules* **1998**, *31*, 3055.
- Borgström, J.; Quist, P–O.; Piculell, L. *Macromolecules* **1996**, *29*, 5926.
- Waigh, T. A.; Kato, K. L.; Donald, A. M.; Gidley, M. J.; Clarke, C. J.; Riekel, C. *Stärke/Starch* **2000**, *52*, 450.
- LeBail, P.; Bizot, H.; Ollivon, M.; Keller, G.; Bourgaux, C.; Buleon, A. *Biopolymers* **1999**, *50*, 99.

- (69) Gessler, K.; Uson, I.; Takaha, T.; Krauss, N.; Smith, S. M.; Okada S.; Sheldrick, G. M.; Saenger, W. *Proc. Natl. Acad. Sci. U.S.A.* **1999**, *96*, 4246.
- (70) Rochas, C.; Brulet, A.; Guenet, J-M. *Macromolecules* **1994**, *27*, 3830.
- (71) Lopez, D.; Saiani, A.; Guenet, J-M. *J. Therm. Anal.* **1998**, *51*, 841.
- (72) Ramzi, M.; Rochas, C.; Guenet, J-M. *Macromolecules* **1998**, *31*, 6106.
- (73) Liang, J. N.; Stevens, E. S. *Biopolymers* **1979**, *18*, 327.
- (74) Burchard, W. *Biomacromolecules* **2001**, *2*, 342.
- (75) Guenet, J-M. *Thermochim. Acta* **1996**, *284*, 67.
- (76) Aberle, T.; Burchard, W. *Stärke/Starch* **1997**, *49*, 215.
- (77) Vesterinen, E.; Suortti, T.; Autio, K. *Cereal Chem.* **2001**, *78*, 442.
- (78) Lauritzen, J. I.; Hoffman, J. D. *J. Appl. Phys.* **1973**, *44*, 4340.
- (79) Khoury, F.; Passaglia, E. In *Treatise on Solid State Chemistry*; Hannay, N. B., Ed.; Plenum: New York, 1976; pp 466–472.
- (80) Bassett, D. C. *Macromol. Symp.* **2004**, *214*, 5.
- (81) Takahashi, Y.; Kumano, T.; Nishikawa, S. *Macromolecules* **2004**, *37*, 6827.
- (82) Imberty, A.; Perez, S. *Biopolymers* **1988**, *27*, 1205.
- (83) Kim, O.-K.; Je, J.; Baldwin, J. W.; Kooi, S.; Pehrsson, P. E.; Buckley, L. J. *J. Am. Chem. Soc.* **2003**, *125*, 4426.

BM050766X